JOINT EUROPEAN TORUS

JET–P(92)33

P.E. Stott
and JET Team

Recent Developments of Diagnostics at JET

Recent Developments of Diagnostics at JET

P.E. Stott
and JET Team*

JET-Joint Undertaking, Culham Science Centre, OX14 3DB, Abingdon, UK

* *See Annex*

Preprint of Paper to be submitted for publication in
Journal of Scientific Instruments and
Proceedings of the APS Diagnostics Conference, Sallote, 1992

Recent Developments of Diagnostics at JET

P E Stott

JET Joint Undertaking, Abingdon, Oxfordshire, OX14 3EA, UK.

Abstract

Since the first operation of JET in 1983, there has been a considerable program of diagnostic development to keep pace with the requirements of the experimental program. Many diagnostic systems have been upgraded and several new ones have been added. New diagnostics are being built and others modified for the pumped divertor which will come into operation at the end of 1993. A few months ago JET carried out a preliminary experiment with tritium which produced the first significant fusion power (over 1.5 MW) and provided the first real test of diagnostics in a high radiation environment. A more extensive experimental program in tritium is planned for 1995 and 1996.

Introduction

The Joint European Torus (JET) has been operating since 1983. There has been a steady increase in fusion performance from $n_i(0)\bar{\tau}_E T_i(0) \approx 6 \times 10^{19} m^{-3}$ and $T_i(0) \approx 2.6$ keV in 1985 to $n_i(0)\bar{\tau}_E T_i(0) \approx 9.5 \times 10^{20}$ m^{-3} and $T_i(0) \approx 28$ keV in 1991[1]. A few months ago JET carried out a preliminary experiment with tritium which produced significant fusion power (over 1.5 MW) for the first time and captured considerable public interest[2]. More extensive experiments in deuterium-tritium plasmas are planned for later in JET's program.

JET has an extensive set of plasma diagnostics (Table 1) which have been purpose-built to very stringent engineering standards. The detailed specification of diagnostic requirements started in 1979. Some of the basic systems were ready for the first plasma operation in 1983; other systems were brought into operation progressively during the next few years[3]. There has been a considerable program of diagnostic development to keep pace with the requirements of the experimental program. Many diagnostic systems have been upgraded and several new ones have been added. Several new diagnostics are being designed (Table 2) including a major package of new diagnostics for the Pumped Divertor (Table 3) that is scheduled to come into operation in 1993.

Many of the JET diagnostics were built under contract by other fusion laboratories. Overall coordination and stringent interface standards were maintained by the JET "central team" in order to ensure compatibility between the individual elements of the complete set of diagnostics and with other JET subsystems. This experience gained on JET provides a good starting point for ITER diagnostics. It is essential to plan the diagnostics for a major fusion experiment as an integrated measurement system. This can be realized only if the detailed work carried out in separate institutes is coordinated by an experienced central team. The total cost of the JET diagnostics systems has been about 10^8 US$. The effort for the design, manufacture, installation, commissioning and operation of the complete set of diagnostics now totals over 1000 man-years. These figures correspond to at least 10% of the overall cost and effort invested into JET since 1978 and provide a useful guide to the budget and staff numbers that will be required to diagnose ITER.

Diagnostic Engineering

JET's large physical dimensions (the plasma mid-plane is 6 m above the floor level) have required substantial engineering structures for many diagnostic systems. All diagnostic systems, particularly those with vacuum connections to the tokamak, have to be compatible with the extremely high standards of engineering that are specified for all JET machine components. These requirements, combined with the need for tritium compatibility and remote handling, have made it necessary to engineer the JET diagnostic systems to a much greater extent than was the norm for previous generations of fusion experiments.

The recent preliminary tritium experiment provided the first operational test of tokamak diagnostics in a high radiation environment. The high neutron flux produced an effect like a snowstorm on the unshielded CCD cameras that view in-vessel surfaces. There was a complete "white-out" of the picture during the period of peak neutron emission (about 6×10^{17} s^{-1}). In fact the majority of the JET diagnostic systems have been designed from the outset to operate in the more extensive tritium phase that is planned to take place at the end of the JET program. Radiation hardening has been achieved for most systems by placing sensitive components outside the biological radiation shield wall. In many cases this results in transmission distances of the order of 100 m. A few systems that have to be located closer to the torus have localized radiation shields, but these must be massive to produce a significant reduction of the radiation background generated by 14 MeV neutrons. Effective solutions to these problems have been found for most JET diagnostic systems but some diagnostics (for example VUV spectroscopy and X-ray diodes, as well as the CCD cameras that have been mentioned already) could not be sufficiently-well shielded or located too far from the plasma and consequently these systems will be removed for JET's final phase.

Recent Diagnostic Developments

The basic set of diagnostic systems was brought into operation ready for the first plasma operation in 1983. Other systems were brought into operation progressively during the next few years. Many of the original diagnostics have now been upgraded and enhanced in response to changing operational requirements or stimulated by advances in diagnostic techniques. Some systems have even gone through this process several times already. A few systems have been scrapped and many new ones added. In the scope of this short review, it is possible to give only a few examples of recent developments. Other recent diagnostic developments are discussed in papers by other JET authors[4,5,6,7] at this meeting.

The JET LIDAR Thomson scattering system[8] is based on laser ranging principles. It uses a ruby laser pulse whose duration, $\tau_L \approx 300$ ps, is much shorter than the transit time of the light across the plasma (about 7 ns). Thus the time of arrival of the scattered light at the detector can be related to spatial position. The back-scattered light is collected and spectrally analyzed using a series of band-pass interference filters to determine the plasma temperature profile. The number of scattered photons gives the density profile. The spatial resolution, $\delta_L = 0.5\ c\ \sqrt{(\tau_L^2 + \tau_D^2)}$, is determined by the duration of the laser pulse τ_L and the time resolution of the detectors τ_D. The main LIDAR system uses micro-channel plate detectors combined with transient digitizers which have a combined response time $\tau_D \approx 700$ ps. The inherent spatial resolution, after some improvement obtained by deconvoluting the received signal to take account of the response time of the system, is about 10 cm. A system with improved spatial resolution has been developed[9] for the plasma edge using a streak camera which shares the light collection system with the existing LIDAR system. The camera has a streak speed of 75 ps/mm which gives an effective time resolution of about 150 ps when used with a spot size of 2 mm. A filter spectrometer is used to divide the scattered light into three frequency bands which are focused onto three spots on the photo cathode of the streak camera. The laser pulse length has been reduced slightly to 250 ps resulting in a spatial resolution $\delta_L \approx 5$ cm. Density and temperature profiles measured in an H-mode plasma with the new system are compared in figure 1 with profiles measured with the "conventional" LIDAR system. The improved spatial resolution of the new system is clearly seen at the plasma edge where there are steep gradients of density and temperature.

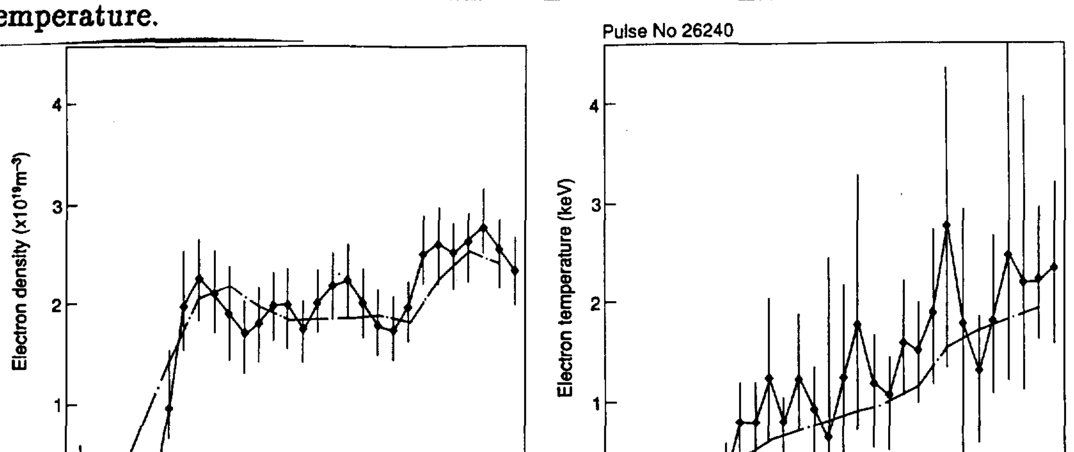

Figure 1: Comparison of density and temperature profiles measured with the high-resolution (full-line) and "conventional" (broken-line) LIDAR systems.

Heterodyne ECE (System KK3 Table 1)

The JET ECE measurement system has several different types of spectrometer. Rapid-scan Michelson interferometers provide measurements of the whole ECE spectrum from which spatial profiles of the electron temperature are derived; a twelve-channel polychromator measures the temperature time dependence with a spatial resolution of about 6 cm; and a heterodyne radiometer measures time-dependent temperatures with spatial resolution of about 3 cm at the plasma edge and about 8 cm in the core. Recently the heterodyne radiometer has been extended to 44 channels covering the frequency ranges 73 to 103 GHz and 115 to 127 GHz in steps of approximately 1 GHz. Different frequency bands can be used simultaneously in different polarizations (ordinary or extraordinary modes) allowing the plasma to be viewed in either the first or second harmonics so that there is almost complete coverage of the plasma cross-section over a wide range of values of toroidal field[10].

The heterodyne system is used for a wide range of studies of temperature transients and fluctuations. In one application[11], the radiometer has been used to measure the edge temperature during the transition from the L-mode to the H-mode. Figure 2a shows that the edge temperature rises in a series of steps as bursts of energy arrive at the edge following a series of sawtooth crashes. The increasing edge temperature causes the frequency of ELMs to fall (figure 2b).

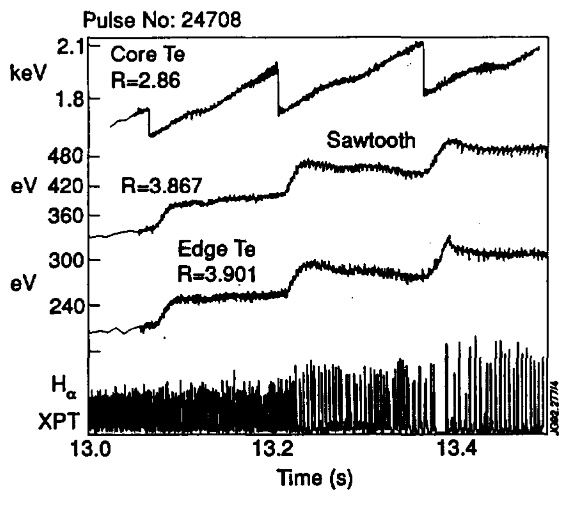

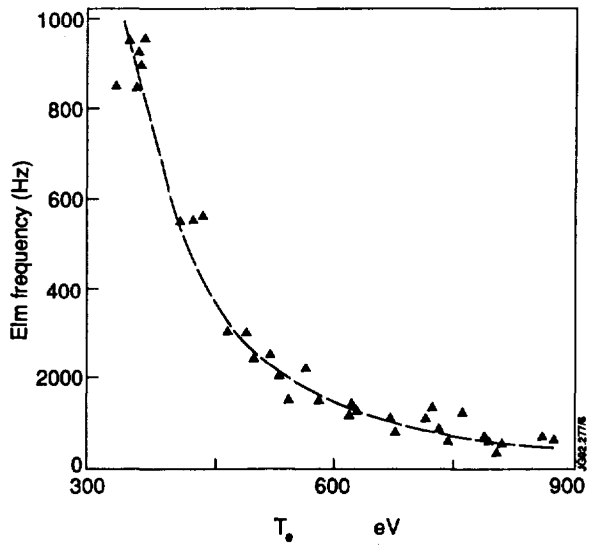

Figure 2a: The two central traces show the temperature at the plasma edge (R = 3.867 and 3.901) measured with the ECE heterodyne system during the transition between the L- and H-modes showing a series of temperature steps coincident with sawtooth crashes (top trace). The bottom trace shows a series of ELMs indicated by spikes in the H_α light from the divertor region.

Figure 2b: Frequency of ELMs versus plasma edge temperature.

Microwave reflectometry (System KG3 Table 1)

Microwave reflectometry has been developed in JET using a multi-channel system which is, in effect, twelve independent reflectometers sharing the same waveguide and antenna system[12]. This arrangement solves the difficulties of sweeping a single reflectometer over a wide frequency range when a long transmission system in oversized waveguide is required to place the sensitive components behind a radiation shielding wall. The twelve sources in the JET system cover the frequency range 18 to 80 GHz corresponding, in the ordinary mode, to the density range 4×10^{18} to 8×10^{19} m^{-3}. Two types of detectors are used: coherent detectors (time resolution ≈ 2 μs) which are sensitive to both amplitude and phase; and fringe counters (time resolution ≈ 10 μs) which measure only the phase. There are two modes of operation: a narrow-band frequency sweep which is used to measure density profiles; and fixed frequencies which are used to follow profile evolution, density transients and density fluctuations. Figure 3 shows a sequence of density profiles measured in the swept-frequency mode during the transition between the L and H-modes. The steepening density gradient at the plasma edge is clearly seen. In the fixed-frequency mode the evolution of the density profile during an ELM can be followed (figure 4).

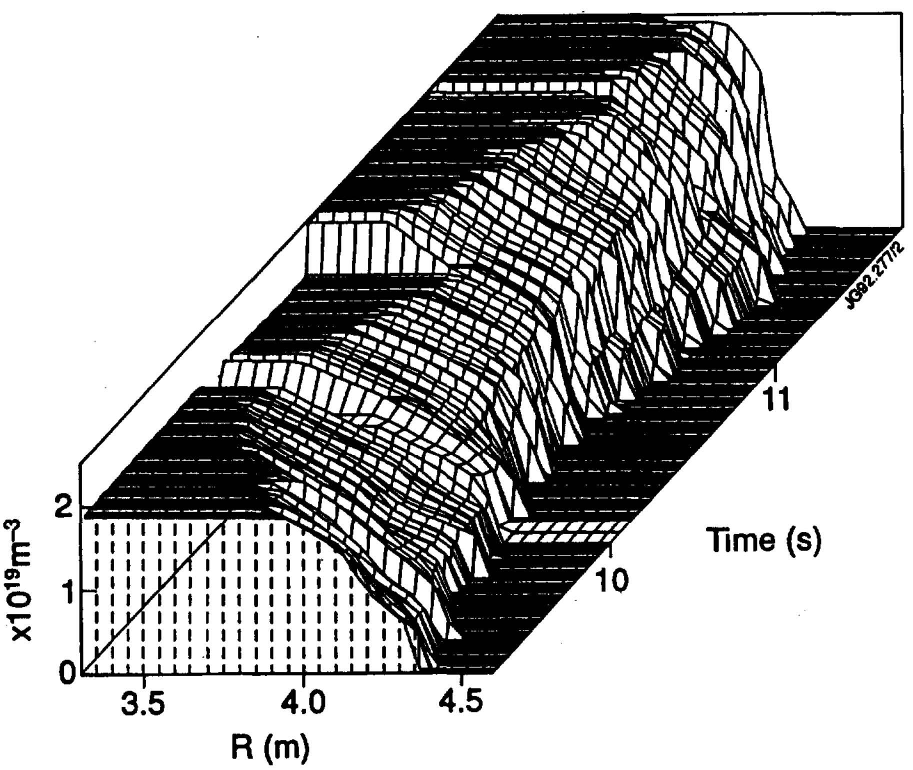

Figure 3: Edge density profiles measured with the reflectometer during the transition between the L- and H-modes.

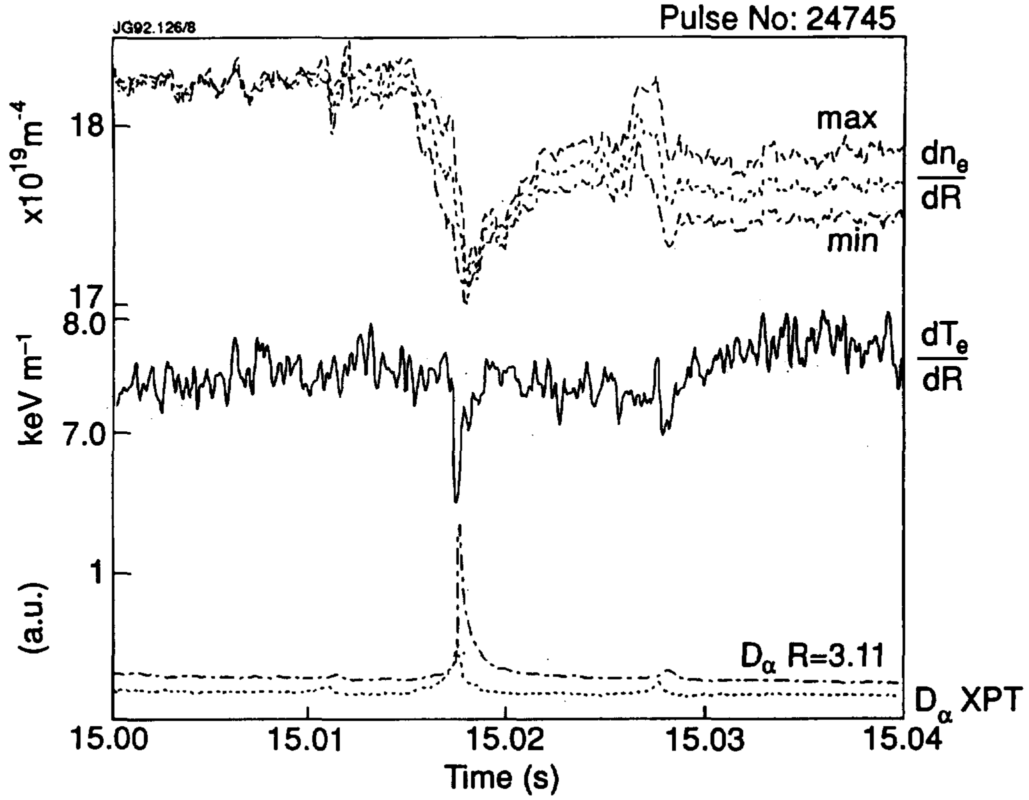

Figure 4: Edge density and temperature gradients during an ELM.

Time–of–flight neutral particle analysis (System KR2 Table 1)

A conventional neutral particle analyzer based on channel multipliers was one of the first JET diagnostics. These detectors are very sensitive to neutrons and this system has become difficult to use as neutron fluxes have risen progressively. A new system using a time-of-flight technique which discriminates against neutrons has been developed and recently commissioned[13]. Neutral particles are ionized in a gas cell and the resulting secondary ions are then energy-analyzed with an electrostatic analyzer as in a conventional system. The ions then pass through a thin carbon foil (1 $\mu g/cm^2$) releasing a secondary electron which is detected by a channel multiplier and starts a coincidence timer. The timer is stopped after a time interval > 50 ns when the ion reaches a second channel multiplier located some 12 to 30 cm away. Spurious counts in either detector due to neutrons fall outside the coincidence window and are rejected. For use during the preliminary tritium experiment, the instrument was surrounded by a radiation shield of water-extended polyethylene and lead in order to reduce the neutron background below the saturation level (about 10^6 Hz) for the channel multipliers. A more substantial shield will be required for the final tritium phase. A typical set of energy spectra for hydrogen, deuterium and tritium is shown in figure 5.

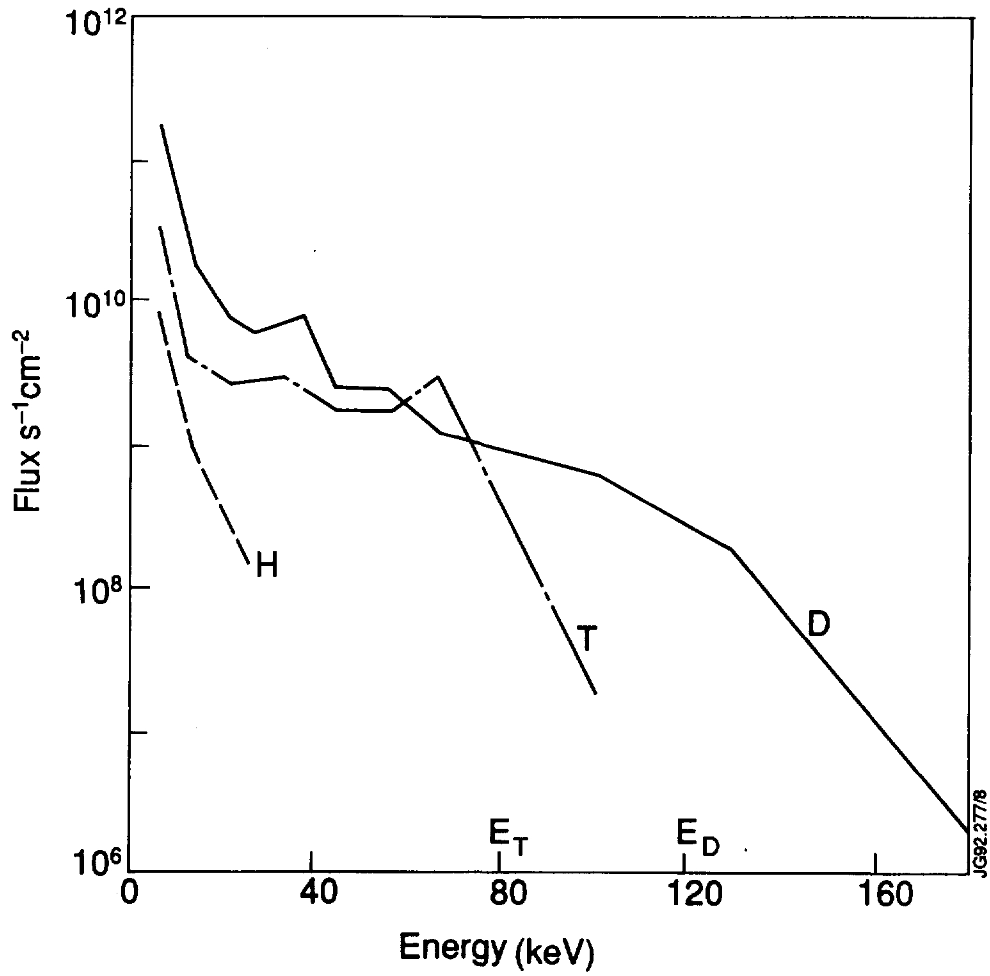

Figure 5: Neutral particle spectra for H, D and T measured with the time-of-flight instrument.

High−energy neutral particles (System KF1 Table 1)

A high-energy neutral particle diagnostic has been developed for JET by the Ioffe Institute with the objective of measuring alpha particles via the double charge-exchange reaction $He^{++} + He^{0} \Rightarrow He^{0} + He^{++}$ with an injected energetic helium neutral beam. This technique is expected to cover alpha particle energies in the range 0.5 to 3.5 MeV. The energetic neutral particles escaping from the plasma are stripped in a thin foil and the secondary ions are energy-analyzed in crossed electric and magnetic fields. They are detected using a thin scintillator which is very sensitive to ions because of their short stopping distance, but relatively insensitive to neutrons which are more penetrating.

The first application of this system has been to study fast hydrogenic ions produced by ion cyclotron resonance heating using the single charge-exchange reaction $H^+ + He^0 \Rightarrow H^0 + He^+$. The flux of passive neutrals before the helium beam is switched on is much larger than expected. Moreover both the active and the passive spectra extend to much higher energies (figure 6) than would be consistent with the charge-exchange process. The expected charge-exchange contribution is recovered by differencing the spectra when normalized at high energy. The enhancement of the spectra is thought to be due to the flux of energetic neutrals produced by radiative recombination or by charge-exchange on impurities. This serendipitous result gives a much stronger flux of high energy neutrals than was expected from charge-exchange with beam particles and offers the prospect of a new diagnostic method.

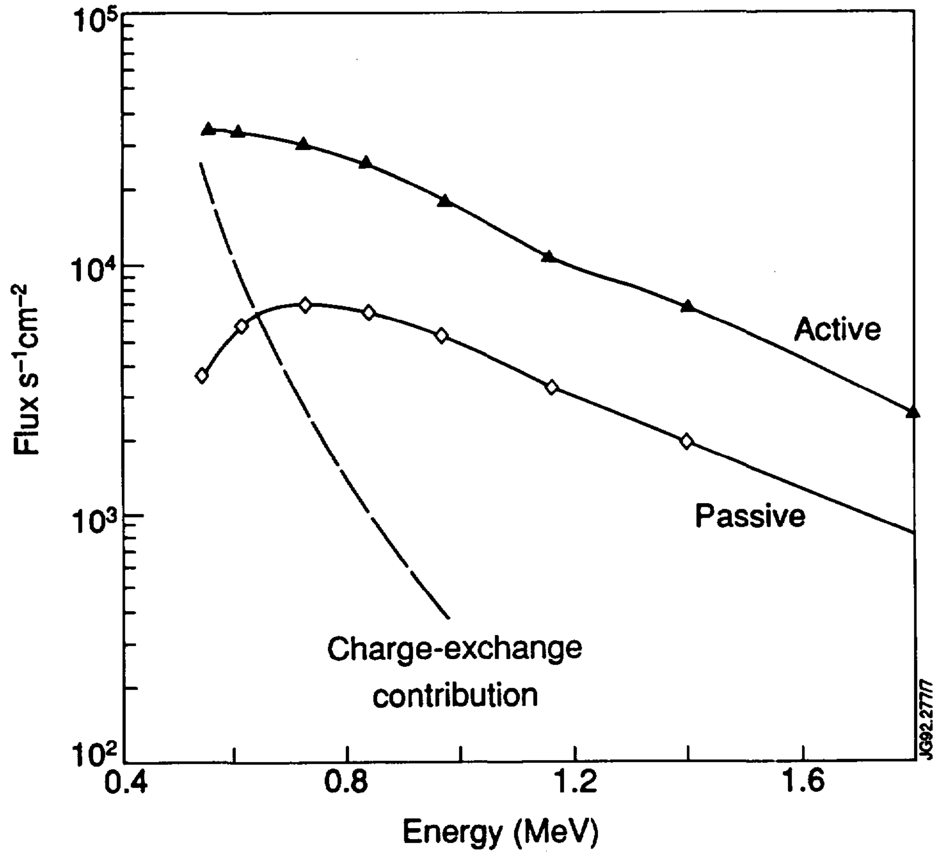

Figure 6: Flux of high-energy neutrals measured with the Ioffe instrument before (passive) and during (active) the injection of a helium neutral beam. The contribution from charge-exchange is shown by the broken line.

Diagnostics for the Pumped Divertor

The highest performance plasmas have been in the X-point configuration with a magnetic separatrix inside the vacuum vessel. During 1991 the upper X-point target was a continuous set of carbon fiber composite tiles and the lower target was a continuous set of beryllium tiles. Both sets of tiles were carefully aligned and shaped to avoid discontinuities. However even with these precautions, the duration of high performance discharges in JET was limited by a high influx of impurities associated with overheating of the limiter or divertor target surfaces, usually referred to as a carbon or beryllium "bloom". This problem must be solved for JET and for ITER and this has motivated the next phase of the JET programme which will be to demonstrate effective methods of impurity control. During 1992 and 1993, the JET tokamak will be extensively modified by installation within the torus vacuum vessel of a pumped divertor. The installation will require substantial modifications to many existing diagnostics as well as the development and construction of several new diagnostics. These new systems (Table 3) are required to provide data about the plasma in the divertor region and in the scrape-off-layer in order to optimize the operation of the divertor, to improve the understanding of divertor physics and to provide a basis for testing plasma boundary models.

The plasma geometry in the divertor X-point region will be determined with magnetic pick-up coils. Fast pressure gauges will be used to determine neutral flows in the divertor. Density and temperature at the divertor target surface will be measured by Langmuir probes in the target plates. A lithium atomic beam diagnostic is planned to measure plasma parameters in the scrape-off layer away from the divertor region.

A new LIDAR Thomson scattering system is being designed to measure density and temperature profiles in the divertor region. The short sampling time inherent in the LIDAR method provides good discrimination against plasma background light. The plasma will be viewed through a port on the vessel mid-plane using an in-vessel mirror. The line-of sight in the divertor region will be close to a line of constant magnetic flux.

Three millimeter-wave diagnostic systems: microwave interferometry; microwave reflectometry; and electron cyclotron absorption, are being developed for electron density and temperature measurements in the pumped divertor region. The three systems will share a common set of waveguides and antennas making use of different polarizations and frequency ranges to separate the instruments. JET already uses interferometry and reflectometry for measurements of the core and scrape-off layer plasmas, but the new systems for the divertor region will have some novel features. The microwave interferometer will use two frequencies in the range 130 to 170 GHz in order to compensate for mechanical movements of the antennas and other components that have to be supported on the vacuum vessel. Heterodyne detection will be used for high sensitivity and in order to measure the direction of the phase change. A broad-band, swept-frequency reflectometer system cannot be used in this application because access to the pumped divertor plasma requires long, oversized waveguides and moreover the complex plasma geometry would give difficulties with interferometric detection. A novel reflectometer system is being developed in order to determine the peak density along the line of sight. A range of fixed frequencies will be launched into the plasma and the highest reflected frequency determined. The level of fluctuations on reflected signals is characteristically different compared to the level on transmitted signals so that the reflected signals can be distinguished easily. A prototype system has been built and operated on JET during the past year. Electron cyclotron emission cannot be used in the divertor plasma because the plasma will not be optically thick and therefore the local ECE emission will be dominated by emission at the same frequency from the much hotter plasma core. The electron cyclotron absorption technique will be used to give a local measurement of the product of density and temperature at the position of the cyclotron resonance.

A major aim of the pumped divertor is to study the dependence of impurity production and retention on edge and divertor parameters. Some of the existing spectroscopic diagnostics are being modified including the VUV spectrometer system which spatially scans the plasma poloidal cross-section via rotating, grazing-incidence mirrors will be upgraded with improved mirrors that will improve the scan time to 25 ms for a complete poloidal scan. The divertor plasma will be viewed from two angles: from the torus mid-plane using an existing spectrometer; and vertically using a new spectrometer. A new double SPRED survey spectrometer covering the wavelength range 10 to 150 nm will be The divertor plasma will be viewed toroidally in both co- and counter directions with a visible light diagnostic in order to determine flow velocities in the divertor. Periscope viewing systems located through gaps in the divertor plates will provide two-dimensional spatial distributions of impurity emission lines.

Summary

The original set of diagnostics that was planned for JET over 10 years ago has proved reliable and capable of extension and modification in response to new requirements and developments of new diagnostic techniques. Most systems have been upgraded and enhanced and several completely new systems have been added.

Acknowledgements

The work reviewed in this paper represents the work of many of my colleagues. In particular I am grateful to A E Costley, A Gondhalekar and M Petrov for help in preparing this paper.

References

1 The JET Team, in *Plasma Physics and Controlled Nuclear Fusion Research 1990* (Proc. 13th Int. Conf. Washington, DC 1990), Vol 1, IAEA, Vienna (191) 27.

2 The JET Team, *Nuclear Fusion* **32** (1992) 187

3 Stott P E, *Phil. Trans. R. Soc. Lond.* A **322** (1987) 47.

4 Zolfaghari A, paper D8 This meeting

5 Machuzak J S, Paper D21 this meeting

6 Jarvis O N, Paper A3 this meeting

7 von Hellermann M, Paper M3 this meeting

8 Salzmann H *et al*, *Rev Sci Instrum* **59** (1988) 1451-1456

9 Fajemirokun H *et al* in *Diagnostics for Contemporary Fusion Experiments* editors Stott P E *et al* Società Italina di Fisica (1991) 853.

10 Porte L, *Doctoral Thesis,* University of Strathclyde, UK also Porte L, Bartlett D V, Campbell D J, and Costley A E, *Controlled Fusion and Plasma Physics (Proc.18th European Conf. Berlin)* Europhysics Conf. Abstracts vol 15C part IV 357.

11 Colton A L *et al, J. Nucl. Mat.* (to be published)

12 Prentice R, Sips A C C, Fessey J A and Costley A E, *Proc 17th European Conference on Controlled Fusion and Plasma Heating,* **14B** part IV, 1500, Amsterdam (1990).

13 Corti S *et al*, in *Diagnostics for Contemporary Fusion Experiments,* Società Italiana di Fisica (1991) 477.

Table 1
Status of JET Diagnostic Systems, December 1991
Operational Diagnostics

System	Diagnostic	Purpose	Association	Automation
KB1	*Bolometer array*	*Time and space resolved total radiated power*	*IPP Garching*	A
KB2X	X-point bolometer	Time and space resolved power from X-point region	JET and IPP Garching	A
KC1	Magnetic diagnostics	Plasma current, loop volts, plasma position, shape of flux surfaces, diamagnetic loop, fast MHD	JET	A
KE3	Lidar Thomson scattering	T_e and n_e profiles	JET and Stuttgart University	A
KE5	q-profile Thomson scattering	Measurement of q-profile	JET	SA
KF1	High energy neutral particle analyser	Ion energy distribution up to 3.5MeV	Purchased from Ioffe St Petersburg	SA
KG1	Multichannel far infrared interferometer	$\int n_e ds$ on six vertical chords and two horizontal chords	CEA Fontenay-aux-Roses	SA
KG3	Microwave reflectometer	n_e profiles and fluctuations	JET and FOM Rijnhuizen	A
KG4	Polarimeter	$\int n_e B_p ds$ on six vertical chords	JET and CEA Fontenay-aux-Roses	SA
KH1	Hard X-ray monitors	Runaway electrons and disruptions	JET	A
KH2	X-ray pulse height spectrometer	Monitor of T_e, impurities, LH fast electrons	JET	SA
KJ1*	Soft X-ray diode arrays	MHD instabilities and location of rational surfaces	IPP Garching	SA
KJ2*	Toroidal soft X-rays	Toroidal mode numbers	JET	SA
KK1	Electron cyclotron emission spatial scan	$T_e(r,t)$ with scan time of a few milliseconds	NPL, UKAEA *Culham and JET*	A
KK2	Electron cyclotron emission fast system	$T_e(r,t)$ on microsecond time scale	FOM Rijnhuizen	A
KK3	Electron cyclotron emission heterodyne	$T_e(r,t)$ with high spatial resolution	JET	SA
KL1*	Limiter viewing	Monitor hot spots on limiter, walls, RF antennae, divertor target tiles	JET	A
KL3	Surface temperature	Surface temperature of target tiles	JET	M
KM1	2.4MeV neutron spectrometer	Neutron spectra in D-D discharges, ion temperatures and energy distributions	UKAEA Harwell	SA
KM3	2.4MeV time-of-flight neutron spectrometer		NEBESD Studsvik	A
KM7	Time-resolved neutron yield monitor	Triton burning studies	JET and UKAEA Harwell	A
KN1	Time-resolved neutron yield monitor	Time resolved neutron flux	UKAEA Harwell	A
KN2	Neutron activation	Absolute fluxes of neutrons	UKAEA Harwell	SA
KN3*	Neutron yield profile measuring system	Space and time resolved profile of neutron flux	UKAEA Harwell	A
KN4	Delayed neutron activation	Absolute fluxes of neutrons	Mol	A
KR2	Active phase NPA	Ion distribution function, $T_i(r)$	ENEA Frascati	A
KS1	Active phase spectroscopy	Impurity behaviour in active conditions	IPP Garching	SA
KS2*	Spatial scan X-ray crystal spectroscopy	Space and time resolved impurity profiles	IPP Garching	SA
KS3	H-alpha and visible light monitors	Ionisation rate, Z_{eff}, impurity fluxes from wall and limiter	JET	SA
KS4	Charge exchange recombination spectroscopy (using heating beam)	Fully ionized light impurity concentration, $T_i(r)$, rotation velocities	JET	SA
KS5	Active Balmer α spectroscopy	T_D, n_D and $Z_{eff}(r)$	JET	SA
KS6*	Bragg rotor X-ray spectrometer	Monitor of low and medium Z impurity radiation	UKAEA Culham	SA
KS7*	Poloidal rotation	Multichannel spectroscopic measurement of poloidal rotation	UKAEA Culham	M
KT1*	VUV spectroscopy spatial scan	Time and space resolved impurity densities	CEA Fontenay-aux-Roses	A
KT2*	VUV broadband spectroscopy	Impurity survey	UKAEA Culham	A
KT3	Active phase CX spectroscopy	Fully ionized light impurity concentration, $T_i(r)$, rotation velocities	JET	SA
KT4*	Grazing incidence + visible spectroscopy	Impurity survey	UKAEA Culham	A
KX1	High resolution X-ray crystal spectroscopy	Central ion temperature, rotation and Ni concentration	ENEA Frascati	A
KY2	Surface probe fast transfer system	Plasma wall and limiter interactions including release of hydrogen isotope recycling	UKAEA Culham	Automated, but not usually operated unattended
KY3*	Plasma boundary probes	Vertical probe drives for reciprocating Langmuir and surface collector probes	JET, UKAEA Culham and IPP Garching	
KY4	Fixed Langmuir probes (X-point belt limiter)	Edge parameters	JET	SA
KZ3*	Laser injected trace elements	Particle transport, T_i, impurity behaviour	JET	M
Kγ1	Gamma-rays	Fast ion distribution	JET	M

* Not compatible with tritium A=Automatic; SA=Semi-automatic; M=Manual

Table 2
Additional Diagnostics under Construction

System	Diagnostic	Purpose	Association	Status
KE4	Fast ion and alpha-particle diagnostic	Space and time resolved velocity distribution	JET	Under construction
KE7	Lidar Thomson scattering	Higher spatial resolution, n_e and T_e in plasma edge	JET	Being tested
KJ3	Compact soft X-ray cameras	MHD instabilities, plasma shape	JET	Design
KJ4	Compact soft X-ray camera	Toroidal mode number determination	JET	Design
KM2	14MeV neutron spectrometer	Neutron spectra in D-T discharges, ion temperatures and energy distributions	UKAEA Harwell	In installation
KM5	14MeV time-of-flight neutron spectrometer		SERC Gothenberg	In installation
KT3D	Active phase visible and UV spectroscopy	Light impurity concentrations, $T_i(r)$ in divertor and centre	JET	Design
KB4	In-vessel bolometer array	Time and space resolved radiated power	JET	Design

Table 3
Diagnostics for the New Phase of JET

System	Diagnostic	Function	Status
KE9D	LIDAR Thomson scattering	T_e and n_e profiles in divertor plasma	In-vessel design complete, procurement in progress.
KG6D	Microwave interferometer	$\int n_e dl$ along many chords in divertor plasma	In-vessel waveguide design complete, procurement in progress
KG7D	Microwave reflectometer	Peak n_e along many chords in divertor plasma	In-vessel waveguide design complete, ex-vessel microwave design and mockup experiments in progress
KK4D	Electron cyclotron absorption	n_eT_e profile along many chords in divertor plasma	In-vessel waveguide design complete, ex-vessel microwave design and mockup experiments in progress
KD1D	Calorimetry of Mark1 divertor targets	Power balance of divertor plasma	Thermocouple installation awaiting delivery of target tiles
KC1D	Magnetic pickup coils	Plasma geometry in divertor region	Manufacture in progress
KY4D	Langmuir probes in divertor target tiles	n_e and T_e in the divertor plasma	Design completed
KY5D	Fast pressure gauges	Neutral flow in divertor region	Manufacture in progress
KT6D	Poloidal view visible spectroscopy of divertor plasma using a periscope	Impurity influx, 2-D emissivity profile of lines	Periscope and in-vessel components in manufacture. Design of other components and optics in progress
KT5D	Toroidal view visible spectroscopy of divertor plasma from Octant No:7 mid-plane	T_z and V_z, ion temperature and toroidal velocity of impurities	Design in progress. Optics components defined and procurement in progress
KT7D	VUV and XUV spectroscopy of divertor plasma	Impurity influx, ionization dynamics	Spectrometer in manufacture, mechanical design in hand, procurement of electronics and data acquisition in hand
KB3D	Bolometry of divertor region	Power balance of divertor plasma	Design of mechanical interface being finalized. Final tests of detector element in progress. Procurement of electronics and data acquisition in hand.
KY6	50kV lithium atom beam	Parameters of the scrape-off-layer plasma	Concept approved, detailed design in progress